

MIT Open Access Articles

*Minimization of Macrosegregation in
DC Cast Ingots Through Jet Processing*

The MIT Faculty has made this article openly available. ***Please share***
how this access benefits you. Your story matters.

Citation: Wagstaff, Samuel R., and Antoine Allanore. "Minimization of Macrosegregation in DC Cast Ingots Through Jet Processing." Metallurgical and Materials Transactions B 47.5 (2016): 3132–3138.

As Published: <http://dx.doi.org/10.1007/s11663-016-0718-6>

Publisher: Springer US

Persistent URL: <http://hdl.handle.net/1721.1/105503>

Version: Author's final manuscript: final author's manuscript post peer review, without publisher's formatting or copy editing

Terms of use: Creative Commons Attribution-Noncommercial-Share Alike



Manuscript submitted on March 29, 2016

Minimization of macrosegregation in DC cast ingots through jet processing

Samuel R. Wagstaff and Antoine Allanore*

Massachusetts Institute of Technology

Department of Materials Science & Engineering

77 Massachusetts Avenue, Cambridge MA 02139, USA

*corresponding author: allanore@mit.edu

Abstract

With an increase in demand for aluminum alloys, industrial suppliers are seeking to increase the size and speed of casting processes. Unfortunately operating the existing Direct-Chill (DC) process in such conditions tends to enhance metallurgical defects. Perhaps the most recognized of these defects is macrosegregation, whose effects are permanent once the material is solidified. In order to facilitate the expansion of the DC process without increasing the presence of macrosegregation, a novel jet mixing method to distribute the liquid metal is presented. The governing equations for this process are derived and predict the operating parameters necessary to minimize centerline macrosegregation. The results of commercial-scale tests are presented, validating the predictive equations and performance of this process.

Introduction

More than two third of the aluminum produced in the United States is first cast into ingots using the Direct-Chill (DC) process¹, prior to being transformed into sheet, plate, extrusions, or foil. The process, devised in its current version in the 1940's has subsisted thanks to its simplicity, robustness, and wide range of applicability. In spite of its industrial importance, metallurgical defects continue to exist and must be addressed before the process may continue to evolve.

One longstanding quality issue for large castings of aluminum alloys is macrosegregation. Defined as compositional variation visible across the dimension of the casting, this macroscopic defect dictates variations of properties throughout the entire finished product^{2,3}. Compositional variations are perhaps one of the earliest recorded metallurgical defects but their origin and prediction continue to be an active area of research. In spite of a large volume of results, no reliable solution has been proposed to mitigate the deleterious effects of macrosegregation at production-level quantities for DC cast slabs.

Background

The fundamental cause behind macrosegregation is the relative movement of liquid and solid phases during solidification^{4,5}. This relative movement implies that the micro-scale partitioning of solute between liquid and solid phases (microsegregation) translates into large-scale differences in chemical composition (macrosegregation). The movement can be driven by a number of factors, whose magnitude depends not only on casting practice, but also alloy composition, and shape of the transition region (sump)^{4,6}. In the present work, the focus is primarily on the transport and preferential sedimentation of free-moving grains, as justified below.

Commercially cast aluminum alloys tend to solidify as equiaxed grains due to the addition of exogenous nucleation sites (grain refiner). In the slurry region (defined as the region between the liquidus and coherency isotherms⁴) these grains are mobile and can travel short or long

distances depending on convection conditions. The preferential sedimentation of these grains at the bottom of the sump is often considered as the origin of centerline segregation in DC cast ingots^{6,7,8}. Grain sedimentation was one of the first mechanisms proposed for segregation⁹, due to the observation of a duplex structure, characterized by a mixture of coarse and fine cell dendritic grains, near the ingot centerline^{10,11,12,13}. As each position in the sump has a distinct solidification pattern, thus a unique microstructure; the observation of several distinct microstructures suggests differing origins and thermal histories of the grains, which have ultimately been transported to the centerline.

When free moving grains are transported and settle at the bottom of the sump, a fraction of solid phase larger than the targeted equilibrium condition is obtained. In hypoeutectic aluminum alloys (i.e. for the majority of DC products) the solid phase is less rich in solute than the liquid, and a larger fraction of solid results in negative segregation upon solidification (concentration of solute lower than the target). It has been shown, e.g. in the case of AA2024, that such negative segregation dramatically alters the ultimate mechanical properties of cast ingots³. It is then foreseen that preventing the sedimentation of free-moving grains will alter macrosegregation, ultimately reducing property variations in DC cast ingots. Herein, we propose the introduction of a turbulent jet directly into the base of the sump as means to prevent the sedimentation of grains. However, it has been suggested that the introduction of a jet of significant power causes erosion of the sump in billet (round) castings⁴. We therefore propose a method to predict a jet of sufficient power to suspend sedimented grains without causing excess sump erosion for slab casting.

Modeling approach

Transport equation and possible integration into finite-element models. With the assumption that heterogenous nucleation acts as the sole source of grains at the solidifying interface, the conservation of mass provides the governing transport equation in the slurry region (Equation 1). A simplified version of the eulerian transport equation for grains relates a source term for nucleation (N in $\text{m}^{-3}\text{s}^{-1}$) to their density (n, m^{-3}) and the velocity u_t ($\text{m}\cdot\text{s}^{-1}$) of the liquid metal.

$$\frac{\partial n}{\partial t} + \nabla \cdot (u_t \cdot n) = N \quad (1.)$$

Thevoz and Rappaz¹⁴ provide a statistical model for the grain density as a function of the mean undercooling ($\Delta T_N \pm \Delta T_\sigma$) and the maximum grain density, (n_{max}) using a Gaussian distribution:

$$\frac{dn}{d(\Delta T)} = \frac{n_{max}}{\sqrt{2\pi}\Delta T_\sigma} e^{-\frac{1}{2}\left(\frac{\Delta T - \Delta T_N}{\Delta T_\sigma}\right)^2} \quad (2.)$$

The specific parameters of Equation 2 (undercooling terms) can be determined experimentally for a given alloy composition, the type of grain refiner used and the duration of its addition. Each unique undercooling corresponds to a certain nucleation radius given by the Gibbs-Thomson relation.

The nuclei formation and melting in Equation 1 are included in a single source term, N , related to the grain density $n(\Delta T)$ at any given undercooling ΔT via the integration of equation 2:

$$N = \frac{dn}{d(\Delta T)} \cdot \frac{d(\Delta T)}{dt} \quad (3.)$$

An additional condition consists of a steady state grain number density, i.e. that $\frac{\partial n}{\partial t} = 0$ in Equation 1. The transport equation to be solved therefore consists in equating the advective contribution with the nucleation at the interface taking into account the local undercooling. The application of this boundary condition at the solidifying interface can be implemented into a finite-element code to determine the appropriate jet parameters. Such approach remains rather computationally intense, and while it would certainly provide the solution, it does not allow prompt application by practitioners. The desired implementation and full description of the system lends itself more readily to a non-dimensional version of the problem, as presented hereafter.

Non-dimensional model

The eulerian fluid dynamic approach to grain flow and in particular grain erosion on granular surfaces is a topic that has received prior attention, for example with the goal of understanding sediment removal and designing pipe and reactor flow conditions for suspension. A brief review of the relevant governing parameters is provided in Appendix 1. The aforementioned parameters have all been experimentally determined for *horizontal* flow over a *horizontal* granular bed. Nonetheless, we can redefine the corresponding parameters for a jet impinging perpendicularly onto the bed. Figure 1 is a schematic representation of this condition, specifically referenced to the case of solidifying metal, though valid for other fluid/grain relationships. Appendix 1 contains the list of symbols and non-dimensional numbers pertinent to the model, and Appendix 2 provides their stepwise derivation for two-phase flow.

We propose to define the Rouse number for a turbulent jet impacting a bed of particles as:

$$Rs = \frac{U_s}{\kappa U_j} \quad (4.)$$

where U_j is the velocity of the jet at the surface of the granular bed (distance $H_0 - h_0$ from the nozzle). Its value can be determined from the theory of turbulent jets¹⁵. Explicitly, U_j is described as:

$$U_j = U_0 \frac{b_0}{\alpha} \left(H_0 - h_0 + \frac{b_0}{2\alpha} \right)^{-1} \quad (5.)$$

where b_0 is the nozzle radius and U_0 is the mean velocity of the fluid at the nozzle outlet in the bulk fluid, expressed as a function of the volumetric flow rate (Q_0).

$$U_0 = Q_0 / (\pi b_0^2) \quad (6.)$$

H_0 and h_0 represent overall depth of the fluid and the granular bed respectively (See Figure 1). For a turbulent jet, the entrainment constant (α) can be taken to be^{16,17} $\alpha = 0.08$. In the case of DC casting, H_0 is typically taken to be the sump depth measured at the coherency isotherm, because the slurry zone is difficult to probe. Numerous relationships exist for the depth of the

sump as a function of casting parameters, but the authors have found good agreement between that proposed by Myhr¹⁸ and experimental results.

For perfectly spherical particles obeying Stokes law (i.e. grain Reynolds number, $Re_g < 0.1$), Sh (Shield), Rs , and Re_g can be related by:

$$Sh = \frac{1}{18\kappa^2} \frac{Re_g}{Rs^2} \approx 0.33 \frac{Re_g}{Rs^2} \quad (7.)$$

Given the fact that the critical Shields number, Sh_c is related to the granular Reynolds number according to¹⁹ $Sh_c \sim Re_g^{-1/2}$, we can determine that the critical Rouse number scales with the granular Reynolds number following:

$$Rs_c \sim Re_g^{3/4} \quad (8.)$$

The presence of several grains falling together leads to a swarm velocity²⁰, U_{th} , provided by

$$U_{th} = U_s(1 - C_v)^m \quad (9.)$$

where C_v is the volume fraction of solid particles. Assuming Stokes law for grains of less than 70 microns (see Appendix 1, table of symbols), m is a constant function of the grain Reynolds numbers:

$$m = \frac{4.7(1+0.15Re_g^{0.687})}{1+0.253Re_g^{0.687}} \quad (10.)$$

Using equation 5 from reference (8), the volume fraction of sedimented grains can be calculated using the observed solute depletion at the centerline reported in reference (6). C_v is then determined to be of the order of 0.2. Using the modified settling velocity (equations 9 and 10) in equation 8 leads to:

$$Rs_c \sim Re_g^{1/2} \quad (11.)$$

For *horizontal* channel flow, bedload transport is defined by the volume flux of grains per unit width of flow Q . This is then normalized by the grain size and settling speed to give a non-dimensional flux per unit width²¹, \tilde{Q} . Through extensive experiments examining bedload transport of uniform *horizontal* flow over granular beds, empirical relationships have been proposed to relate \tilde{Q} to the difference, $Sh - Sh_c$, following:

$$\tilde{Q} = C_s(Sh - Sh_c)^P \quad (12.)$$

P and C_s are constants dependent upon grain size, density, and the stress imposed by the flow over the bed.

In a study of jet scour, Mazurek and Hossain²² showed that the radius of the crater generated by an impinging jet does not vary significantly with increasing jet power. Extrapolating from this, it

is proposed that the crater deepens while its radius (r_0) is almost constant with increasing jet velocity at the base of the crater. This assumption and extrapolation is likely only valid for cohesion-less grains forming a permeable bed, as found in the slurry region of the sump. In addition, the act of impingement on such bed is assumed to lead to a surface pressure distribution and a seepage flow within the bed²³. This seepage flow allows shear stresses to act deep into the bed. Such assumptions likely do not apply for cohesive granular beds, such as welded grains located in the mushy zone of the sump. For such cohesive bed, one would rely on high-temperature creep effects for the applied shear stress to enable re-suspension. This type of bed tends to “reflect” the impinging jet and thus leads to non-uniform and less predictable grain re-suspension.

With the assumption of a cohesion-less bed and a constant crater radius, the volume flux of grains suspended from the crater due to the jet can be represented as:

$$Q \propto r_0^2 U_c \quad (13.)$$

where the crater descent velocity (U_c) is assumed to be constant, i.e. the volume flux is constant. Similar to statistically steady horizontal flow, a non-dimensionalizing constant can be defined by the granular settling flux divided by the across-flow granular density:

$$\frac{d_g^2 U_{th}}{\left(\frac{d_g}{r_0}\right)^2} \quad (14.)$$

In this definition we have used the hindered settling velocity to account for inter-granular interactions within the crater. Equation 14 then allows defining the non-dimensional volume flux as:

$$\tilde{Q} = \frac{U_c}{U_{th}} \quad (15.)$$

This relationship defines the “relative crater descent velocity”, suggesting that the crater descends independently of the properties of the grains themselves.

Because the definition of Rs (equation 4) explicitly invokes the settling velocity of the grains and thus can account for the influence of turbulent fluctuations, we propose to replace equation 12 with a non-dimensional flux of grains of the form:

$$\tilde{Q} = C_r Re_g (Rs_c - Rs) \quad (16.)$$

Using equations 4, 15 and the relationship for the critical Rouse number (equation 11), equation 16 provides an explicit expression for the crater descent speed U_c as a function of the impacting jet velocity on the bed:

$$U_c \approx C_1 U_{th} Re_g^{3/2} \left(1 - C_2 \frac{U_{th}/U_j}{Re_g}\right) \quad (17.)$$

The optimal jet has sufficient power to re-suspend the sedimented grains, but insufficient power to erode the bottom of the sump. We therefore propose that the crater descent velocity (U_c) shall be equal to the casting velocity, i.e. the vertical speed of displacement of the solid ingot. This criterion guarantees no accumulation of grains in the center of the ingot, and that the power of the jet is dissipated in granular resuspension.

Since the jet velocity at the surface of the granular bed (U_j) is a function of the volumetric flow rate, and thus also the casting velocity, an iterative computational solver is implemented until convergence.

Application of the model

Alloy composition is a key parameter of the model, since it influences both the relative density of the solid phase and the steady-state depth of the sump. Indeed, for DC casting where the majority of the heat is removed through the solidified material, certain elements such as magnesium or zinc drastically influence the sump depth due to their lower thermal conductivity with respect to pure aluminium. Such sump depth differences will clearly affect the extent of the jet expansion. As the centerline velocity of a jet will clearly vary with depth, it is anticipated that different jet diameters are required for different alloy compositions. Using data from reference (24) and Myhr and Hakonsen's sump depth prediction¹⁸, it is possible to provide 'boundary' curves representing the effective processing parameters for minimum centerline segregation for a range of typical aluminium alloys, as shown in Figure 2. This figure represents the range of predicted jet Reynolds numbers as a function of mold Reynolds number, respectively defined as:

$$Re_j = \frac{2M_l M_w U_c}{\pi b_0 \nu} \quad Re_m = \frac{2M_l M_w U_c}{\nu(M_l + M_w)} \quad (18.)$$

where M_l and M_w represent the mold length and width respectively.

The boundary of the shaded region is created for two alloys identified as limiting cases; nearly all other alloys will fall between these boundaries.

Experimental Setup and Procedure

In order to test the proposed model, a series of experiments were designed in order to compare our jet-processed results against existing experimental data on macrosegregation. To that end, we determined Al4.5Cu was the best candidate due to the availability of prior experimental data reported in reference (6). Experimental conditions were identical to those described in references (6) and (25) for each trial, the only difference being that each trial used a distinct jet diameter. Figure 2 represents the predicted jet parameters based on the model predictions and the casting conditions (mold dimensions, casting speed). Based on the predictive plot, the minimum macrosegregation should be observed for Al4.5Cu with a jet characterized by a Reynolds number of approximately 97,000 for a mold Reynolds number of approximately 1600.

Following the casting, cross sections were taken from each of the ingots at a cast length of 1800mm, and then analyzed using an Olympus Alloy Plus XRF Analyzer according to the procedure outlined in reference (31).

Results

Macrosegregation surfaces

Figures 3A-F are surface plots of the top left quadrant of a horizontal section of a slab (seen from the top), showing the relative deviations from furnace composition for the five casting conditions shown in Figure 2.

In reference (6) we noticed that the jet has a significant impact on the macrosegregation profile of an Al4.5Cu ingot, and clear trends are observed. Specifically, ingots cast with a jet Reynolds number below 97000 exhibit positive (enriched) centerline segregation, as opposed to the negative segregation observed for ingots cast without a jet (Figure 3A). In contrast, ingots cast with a jet Reynolds numbers of 97000 (Figure 3E) or above hardly exhibit centerline segregation, and if any a negative (depleted) segregation. In addition, the extent of the centerline region is significantly narrower with respect to the short axis when using a jet, with a few centimeters in thickness compared to tens of centimeters in absence of the jet.

Quantitative analysis

The qualitative analysis of the plots in Figure 3 illustrates the potential for jets to modify centerline segregation in rolling slab ingots. The fact that the centerline segregation zone itself is reduced is a successful outcome of the jet additions, since thermo-mechanical processing of the ingot is foreseen to reduce the remaining segregation. However, in order to perform a more quantitative analysis of the process performance, a metric called the Macrosegregation Index (MI) has been developed to quantify the degree of centerline segregation. Equation 19 is a modified second-area moment equation that assigns quantitative values to the concentration measured at each position, based on its deviation from the target alloy composition and its distance from the center.

$$MI = \frac{1}{C_0} \left[\frac{Y}{A} \iint_A (C - C_0)^2 \frac{1}{Y} dA \right]^{1/2} \quad (19.)$$

Incorporating distance in the metric is important as enriched chill zone, which can be handled by physical means after casting, could skew the analysis of the whole section of the ingot. Since the index includes a squared term, it counts as equally unfavorable positive or negative segregation. The MI will be minimal for the cross section with the least macrosegregation.

Figure 4 is a plot of the MI for each of the jet tests reported above, identified by their jet Reynolds number. The red dashed line represents the MI from the standard DC profile analyzed in reference (6) and reproduced in Figure 3A. For the range of jet diameter tested, the macrosegregation index shows at least a 30% reduction from the standard casting method. The best performing jet, (Re=97000) allows a 60% reduction in centerline segregation, confirming the validity of the quantitative model presented above.

Conclusion

A new liquid distribution method, based on an impinging jet, capable of significantly reducing centerline segregation even in large castings, has been proposed. A dimensionless model of the distribution of the molten metal has been proposed, applicable in principle to nearly all alloys and mold dimensions. The model quantitative predictions for casting Al4.5Cu

rolling slab ingots have been validated experimentally at industrial scale, confirming the existence of an optimal jet to minimize centerline segregation. Further work is required to better understand the flexibility and robustness of the model with respect to each of the major process parameters (alloy, amount of grain refinement etc.).

As demonstrated in reference 25, such method can result in a drastic reduction in grain size, indicating the value of future studies of the effect of the impinging jet on dendrite fragmentation, and potency of grain refiners.

Appendix 1

α	Entrainment constant (0.08)	n_{max}	Maximum number density of grains
ΔT	Undercooling	N	Nucleation source term
ΔT_N	Mean undercooling	Q	Volume flux of grains
ΔT_σ	Standard deviation of undercooling	Q_0	Volumetric flow rate
κ	von Kármán constant (0.41)	\tilde{Q}	Nondimensional particle flux per unit width
ν	Kinematic viscosity ($5.5 \times 10^{-7} \text{ m}^2/\text{s}$)	r_0	Crater radius
ρ_f	Fluid density	Re_g	Grain Reynolds number
ρ_g	Grain density	Re_j	Jet Reynolds number
b_0	Nozzle radius	Re_m	Mold Reynolds number
C	Composition	Rs	Rouse number
C_0	Furnace composition	Rs_c	Critical Rouse number
C_v	Volume fraction of grains	Sh	Shields parameter
d	Grain diameter (<70 μm)	Sh_c	Critical Shields parameter
h_0	Depth of bed	u_t	Velocity through control volume
H_0	Depth of fluid and bed	u_*	Shear velocity
m	Exponential constant	U_0	Velocity of jet at nozzle
M_l	Mold length	U_c	Casting Speed/Crater descent speed
M_w	Mold width	U_j	Velocity of jet at bed
MI	Macrosegregation Index	U_s	Stokes settling velocity
n	Number density of grains	U_{th}	Hindered settling velocity

Appendix 2

In studies of uniform, statistically steady turbulent flow over a granular bed, the suspension and transport of particles is generally characterized by the Shields parameter, Sh , representing the ratio of shear stress due to fluid flow relative to the weight per area of individual grains inside the bed²⁶. This has been displayed below in Eq 4, where U is the characteristic flow velocity, d_g , grain diameter, and ρ_f and ρ_g the fluid and grain densities respectively.

$$Sh = \frac{\rho_f U^2}{g(\rho_g - \rho_f) d_g} \quad (20.)$$

Transport of grains occurs if the Shields parameter exceeds a critical value, which depends on grain size, shape, cohesion and buoyancy^{27,28,29}. This critical Shields parameter can be difficult to determine experimentally^{30,31}, partially because the physical mechanism for resuspension occurs transiently due to turbulent fluctuations.

An alternative classification of granular resuspension and sedimentation is expressed by the Rouse number, Rs , which is proportional to the ratio of the settling speed of the grains, and the turbulent shear velocity of the bed. This relation is expressed below in Equation 5 where u_* is the shear velocity, $\kappa = 0.41$ is the von Kármán constant, and U_s is the terminal settling velocity of the grains.

$$Rs = \frac{U_s}{\kappa u_*} \quad (21.)$$

Below a critical value of Rs , the flow is capable of maintaining grains in suspension because turbulent velocity fluctuations are larger than the terminal velocity of each grain. In unidirectional, steady flow, full bed transport is anticipated for $Rs \leq 2.5$, and significant resuspension occurs if $Rs \leq 1$. Unlike the Shields number, the Rouse number accounts for the influence of viscosity upon each particle through the value of its respective settling speed, U_s . For very small grains ($<70 \mu\text{m}$ in the aluminum system) U_s is given by the Stokes settling velocity, U_s .

$$U_s = \frac{g(\rho_p - \rho_f)d^2}{18\nu\rho_f} \quad (22.)$$

The granular Reynolds number (Re_g) is most usefully defined using U_s as the characteristic velocity, thereby forming:

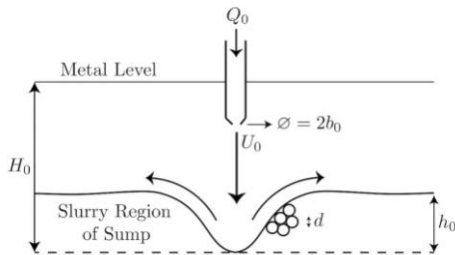
$$Re_g = \frac{U_s d_g}{\nu} \quad (23.)$$

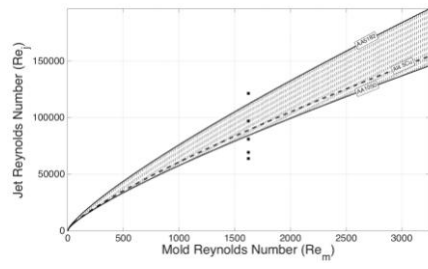
where d_g is the grain diameter, and ν is the kinematic viscosity (generally assumed to be approximately $5.5 \times 10^{-7} \text{ m}^2/\text{s}$ for molten aluminum).

Acknowledgements

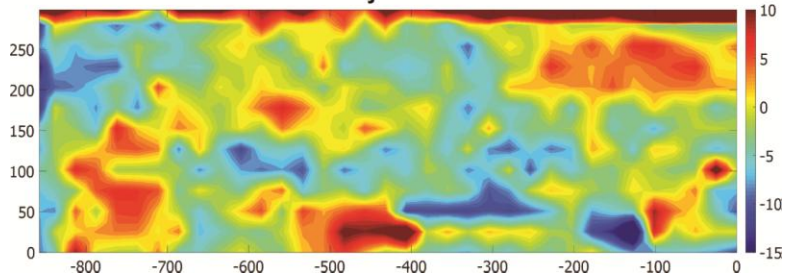
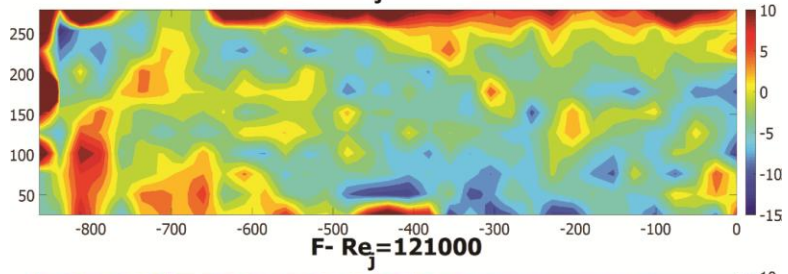
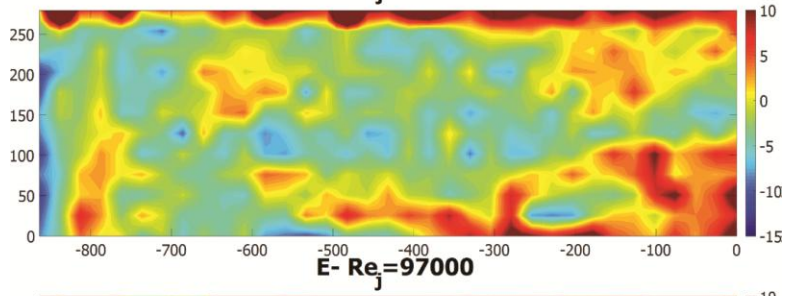
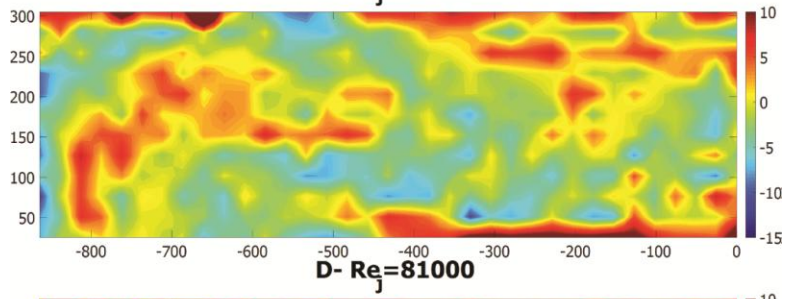
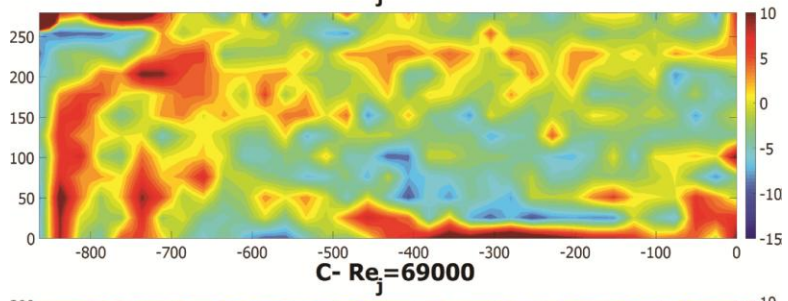
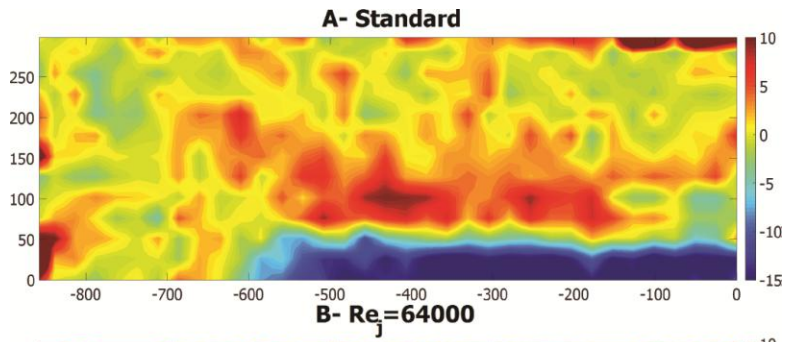
The authors thank the Novelis Solatens Technology Center for their invaluable assistance in completing the present work, and their continuous support.

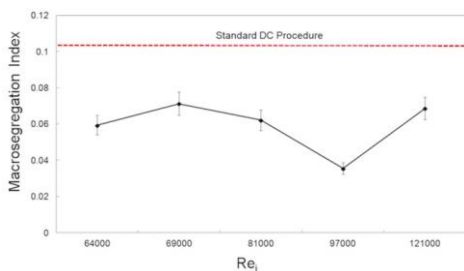
References





351





PLEASE TYPE

Metallurgical and Materials Transactions

AUTHOR INFORMATION FORM

The printer uses the information on this form in the AUTHOR BOX and for contacting the author concerning proofs. Please complete the form carefully.

MANUSCRIPT NUMBER:

Your proofs will be sent as a PDF file, viewable and printable using the free Adobe Acrobat program. When ready, these password protected proofs will be posted to the World Wide Web, and you will be contacted with instructions for accessing and viewing them.

:E-TP-16-312-BR
the Internet.

Your proofs will be sent electronically via

will

(Your e-mail address is necessary. You

proofs.)

receive instructions for viewing your

Proofs are normally ready within 6-8 weeks after the printer receives the manuscript. Please be sure to make arrangements for checking of proofs if you expect to be away from your office for any length of time. Delay in return of proofs will delay publication of the article.

Please note that artwork will be published in color in the online version for free. If you wish to publish color artwork in the hard-copy version, the price will be \$1150 per article with print color artwork. Please check off one of the following:

☐ The article has no color artwork.

☒ The color artwork should be printed in black and white.

☐ The color artwork should be printed in color; I understand there is an additional cost.

NAME OF CORRESPONDING AUTHOR: Antoine Allanore

TELEPHONE: 617 803 8304

FAX: 617 253 5418

E-MAIL: allanore@mit.edu

NAME, PRESENT POSITION, AND AFFILIATION OF ALL AUTHORS **INCLUDING CORRESPONDING AUTHOR** (LIST EACH NAME SEPARATELY):

(First) Samuel R. Wagstaff, Graduate Student, Massachusetts Institute of Technology
Department of Materials Science & Engineering
77 Massachusetts Avenue, Cambridge MA 02139, USA

(Corresponding) Antoine Allanore, T.B. King Assistant Professor of Metallurgy,
Massachusetts Institute of Technology
Department of Materials Science & Engineering
77 Massachusetts Avenue, Cambridge MA 02139, USA

¹ The Aluminium Association, *Aluminum Industry Technology Roadmap*, Washington D.C., May 1997.

² L. Swartzendruber, L. Ives, W. Boettinger, S. Covcill, D. Ballard, D. Laughlin, R. Clough, F. Biancello, P. Blau, J. Cahn, R. Mehrabian, G. Free, H. Berger and L. Mordfin. Report PB81-172348, National Bureau of Standards, National Measurement Lab. Washington D.C., December 1980.

³ L. Ives, L. Swartzendruber, W. Boettinger, M. Rozen, S. Ridder, F. Biancello, R. Reno, D. Ballard, R. Mehrabian. Internal Report 83-2669. National Bureau of Standards. Washington D.C., January 1983.

⁴ D.G. Eskin: *Physical Metallurgy of Direct-Chill Casting of Aluminum Alloys*, CRC Press, Boca Roton, FL, 2008.

⁵ M.C. Flemings: *ISIJ Intern.*, 2000, vol. 40, pp. 833–841.

⁶ S.R. Wagstaff and A. Allanore: *Light Metals*, TMS, 2015, pp. 877-882.

⁷ H. Yu, D.A. Granger, *Int. Conf. Aluminum Alloys—Their Physical and Mechanical Properties*, Charlottesville, VA. EMAS, Warley (U.K.), 1986, pp. 17–29.

⁸ M.G. Chu, J.E. Jacoby: *Light Metals*, TMS, 1990, pp. 925-930.

⁹ S.M. Voronov. *Z. Metallkde.*, 1929, vol. 21, p. 310.

¹⁰ A. Håkonsen, D. Mortensen, S. Benum, H.E. Vatne: *Light Metals*, TMS, 1999. pp. 821–827.

¹¹ Suyitno, D.G. Eskin, V.I. Savran, L. Katgerman. *Metall. Mater. Trans. A*, 2004, vol. 35A, pp. 3551–3561.

¹² D.G. Eskin, V.I. Savran, L. Katgerman: *Metall. Mater. Trans. A*, 2005, vol. 36A, pp. 1965–1976.

¹³ R.K. Nadella, D.Eskin, L. Katgerman: *Continuous Casting of Non-ferrous Metals*, Neu-Ulm, Germany, Weinheim: Wiley-VCH, 2005, pp. 277–282.

¹⁴ P.Thevoz, J.L. Desbioles, M.Rappaz: *Metall. Trans. A*, 1989, vol. 20A, pp. 311-22.

¹⁵ B. R. Morton, G. I. Taylor, and J. S. Turner: *Proc. R. Soc. London*, 1956, Ser. A 234, pp. 1–23.

¹⁶ B. R. Morton, *J. Fluid Mech.*, 1959, vol. 5, pp. 151–163.

¹⁷ N. Kaye: *Atmos.-Oceans.*, 2008, vol. 46, pp. 433–441

¹⁸ A. Myhr and O. R. Hakonsen: *Cast Metals*, 1995, vol. 8, pp. 147-157.

¹⁹ R. J. Munro, N. Bethke, and S. B. Dalziel: *Phys. Fluids*, 2009, vol. 21, 046601.

²⁰ J.F. Richardson, W.M. Zaki: *Trans. Instn Chem. Engrs.*, 1954, vol. 32, pp 35.

²¹ L. van Rijn: *J. Hydraul. Eng.*, 1984, vol. 110, pp. 1431–1456.

²² K. Mazurek and T. Hossain: *Can. J. Civ. Eng.*, 2007, vol. 34, pp. 744-751.

²³ H. Kobus, P. Leister & B. Westrich: *J. Hydr. Res.*, 1979, vol. 17, pp. 175–192.

²⁴ J.R. David (Editor): *ASM Specialty Handbook- Aluminum and Aluminum Alloys*. ASM International. Materials Park, OH. 1993.

²⁵ S.R. Wagstaff, and A. Allanore: *Light Metals*, TMS, 2016, pp. 715-720.

²⁶ A. Shields: *Anwendung der Aehnlichkeitsmechanick und der Turbulenzforschung auf die Geschiebebewegung*, Mitt. Preuss. Vers. Wasser. Schiff. 1936.

-
- ²⁷ B. M. Sumer, L. H. C. Chua, N.-S. Cheng, and J. Fredsøe: J. Hydraul. Eng., 2003, vol. 129, pp. 585–596.
- ²⁸ S. A. Miedema: J. Dredging Eng., 2012, vol. 12, pp. 1–49.
- ²⁹ S. A. Miedema: J. Dredging Eng., 2012, vol. 12, pp. 50–92.
- ³⁰ B. Gomez: Earth-Sci. Rev., 1991, vol. 31, pp. 89–132.
- ³¹ Y. Niño, F. Lopez, and M. Garcia: Sedimentology, 2003, vol. 50, pp. 247–263.

List of Figure Captions

Figure 1: Schematic of a liquid metal jet with volume flux Q_0 , impinging on a granular bed through a nozzle of radius b_0 . The velocity of the jet exiting the nozzle is U_0 . The jet is situated a height, H_0 above the coherency isotherm. Above this is a granular bed (grain diameter d) of material forming the slurry region of height h_0 .

Figure 2: Predictive plot for jet processing parameters. The mold Reynolds number is based on an equivalent hydraulic radius, and casting speed. The jet Reynolds number is based on the jet velocity and diameter. Shaded region represents a range of values dependent on alloy properties. The dashed line represents the prediction for Al4.5Cu. The squares represent the conditions tested on a commercial DC caster.

Figure 3: A-F Surface contours representing deviation from furnace composition as observed in one quadrant of horizontal sections taken at 1800mm of cast length : A- Standard casting procedure B-F using impinging jets of $Re_j = 64000, 69000, 81000, 97000, 121000$. The color code is based on relative deviation from furnace composition (in %), positive values corresponding to solute *enrichment*, while negative values represent solute *depletion*. All X and Y axes are identical with (0,0) representing the center of the cross-section

Figure 4: Macrosegregation index (MI) for each of the experimental jet conditions. The red dashed line represents the MI for a standard DC cast ingot.